Chemico-Biological Interactions 240 (2015) 208–218

Contents lists available at ScienceDirect

Chemico-Biological Interactions

journal homepage: www.elsevier.com/locate/chembioint

Bioactivation of luteolin by tyrosinase selectively inhibits glutathione S-transferase

Rajiv Balyan [a], Shashi K. Kudugunti [b], Hamzah A. Hamad [c], Mohammad S. Yousef [c, d], Majid Y. Moridani [a, e, *]

[a] Department of Pharmaceutical Sciences, School of Pharmacy, Texas Tech University Health Sciences Center, Amarillo, TX 79106, USA
[b] Repligen Corporation, 41 Seyon St, Bldg 1, Suite 100, Waltham, MA 02453, USA
[c] Department of Physics, College of Arts & Sciences, Southern Illinois University, Edwardsville, IL 62025, USA
[d] Biophysics Department, Faculty of Science, Cairo University, Egypt
[e] Clinical Chemistry and Toxicology, Department of Pathology, Medical College of Wisconsin, 9200 W. Wisconsin Avenue, Milwaukee, WI 5322, USA

ARTICLE INFO

Article history:
Received 10 February 2015
Received in revised form
7 July 2015
Accepted 11 August 2015
Available online 14 August 2015

Keywords:
Luteolin
Melanoma
SK-MEL-28
Cancer
Quinone
Glutathione
GST

ABSTRACT

Glutathione S-transferase (GST) plays a significant role in the metabolism and detoxification of drugs used in treatment of melanoma, resulting in a decrease in drug efficacy. Tyrosinase is an abundant enzyme found in melanoma. In this study, we used a tyrosinase targeted approach to selectively inhibit GST. In the presence of tyrosinase, luteolin (10 μM) showed 87% GST inhibition; whereas in the absence of tyrosinase, luteolin led to negligible GST inhibition. With respect to GSH, both luteolin-SG conjugate and luteolin-quinone inhibited ≥90% of GST activity via competitive reversible and irreversible mixed mechanisms with K_i of 0.74 μM and 0.02 μM, respectively. With respect to CDNB, the luteolin-SG conjugate inhibited GST activity via competitive reversible mechanism and competitively with K_i of 0.58 μM, whereas luteolin-quinone showed irreversible mixed inhibition of GST activity with K_i of 0.039 μM. Luteolin (100 μM) inhibited GST in mixed manner with K_i of 53 μM with respect to GSH and non-competitively with respect to CDNB with K_i of 38 μM. Luteolin, at a concentration range of 5–80 μM, exhibited 78–99% GST inhibition in human SK-MEL-28 cell homogenate. Among the 3 species of intact luteolin, luteolin-SG conjugate, and luteoline-quinone, only the latter two have potential as drugs with K_i < 1 μM, which is potentially achievable *in-vivo* as therapeutic agents. The order of GST inhibition was luteolin-quinone >> luteolin-SG conjugate >>> luteolin. In summary, our results suggest that luteolin was bioactivated by tyrosinase to form a luteolin-quinone and luteolin-glutathione conjugate, which inhibited GST. For the first time, in addition to intracellular GSH depletion, we demonstrate that luteolin acts as a selective inhibitor of GST in the presence of tyrosinase. Such strategy could potentially be used to selectively inhibit GST, a drug detoxifying enzyme, in melanoma cells.

1. Introduction

Melanoma is the cancer of melanocytes with propensity of metastasis to other organs. Melanoma accounts for small proportion of all cases of skin cancer, however it is responsible for 75% deaths in skin cancer. In 2014, approximately 76,000 new cases of melanoma and 10,000 melanoma related deaths were expected in US alone (American Cancer Society, 2014).

Based on severity of symptoms, melanoma is divided to four stages. If diagnosed at early stages, melanoma is easily cured. Effective treatment is not available for stage 3 and 4. The available options at later stages include chemotherapeutics, immunotherapy such as interleukin-2, inhibitors of CTLA-4 and PD-1 receptors, inhibitors of signal transduction pathways such as BRAF inhibitor sorafenib [1] and radiation treatment. However these treatments have their limitation and adverse side effects. Only Dacarbazine is approved as a chemotherapeutic by FDA for treatment of melanoma and it is not very effective in preventing metastasis or enhancing survival [2]. After a patient is diagnosed with metastatic

Abbreviations: MEMα, Modified Eagle Medium Alpha; FBS, fetal bovine serum; PBS, phosphate buffered saline; MEM, minimum essential medium; DETAPAC, diethylenetriaminepentaacetic acid; GST, glutathione S-transferase; MRP, multidrug resistance proteins; GSH, glutathione; MDR, multi drug resistance; CDNB, 1-chloro-2,4-dinitrobenzene; DTNB, 2-nitro-5-thiobenzoic acid; 4-HA, 4-hydroxyanisole.

* Corresponding author. Chemistry and Toxicology, Department of Pathology, Medical College of Wisconsin, Milwaukee, WI 53226, USA.
E-mail address: mmoridani@mcw.edu (M.Y. Moridani).

http://dx.doi.org/10.1016/j.cbi.2015.08.011
0009-2797/

melanoma, survival period is only 6–9 months. There is an urgent need of effective drug against melanoma with minimal adverse effects.

Tyrosinase enzyme is abundantly present in melanocytes (2000 fold compared with normal cells) and converts flavonoid to quinone intra-cellularly which is toxic towards melanoma cells. Hence, tyrosinase is considered an excellent target for prodrug therapy specific for melanoma [3–5]. Flavonoids are polyphenolic compounds capable of modulating the activity of many enzymes such as telomerase [6], histidine decarboxylase [7], cyclo-oxygenase, lipooxygenase, phospholipase A2 [8]. Some of flavonoids can also inhibit detoxifying enzymes such as cytochrome P450 enzymes, sulphotransferase, glucuronosyltransferase [9] and glutathione-S-transferase [10,11].

Being a detoxifying enzyme, GST can remove xenobiotics as well as anti-cancer drugs from malignant cells, contributing to drug-resistance. The expression and activity of GST-π is multifold higher in melanoma cells [12]. The GST is responsible for inactivating active drug species. Hence, an ideal drug for melanoma should be selectively toxic to melanoma cells by selectively inhibiting GST in the presence of tyrosinase.

Luteolin (3′,4′,5,7-tetrahydroxyflavone) is present in various dietary sources such as vegetables, fruits, vegetable oils, wines, tea etc. It possess a catechol group (two adjacent –OH groups on ring C, see Scheme 1) which can be converted to quinone in presence of tyrosinase. Recent studies have reported various mechanisms of anti-cancer effect of luteolin. It is reported to inhibit epithelial mesenchymal transition in melanoma and regulate β3 integrin. In other studies luteolin was reported to regulate many other signaling pathways and induction of apoptosis [13,14]. For instance, luteolin can inhibit PI3K/Akt/mTor and MAPK pathways, which are major survival pathways in many cancers including melanoma [15,16]. All these properties make luteolin potentially a good candidate as an antineoplastic agent. Current study is aimed at assessing inhibition of GST by luteolin and the extent of GST inhibition in the presence of tyrosinase. Because luteolin is a substrate for tyrosinase, we used a tyrosinase targeted approach to selectively inhibit GST. The nature of GST inhibition; competitive, non-competitive or mixed and reversibility of inhibition were also investigated. Time- and dose-dependent inhibition of GST and inhibition of GST present in melanoma cells were also studied.

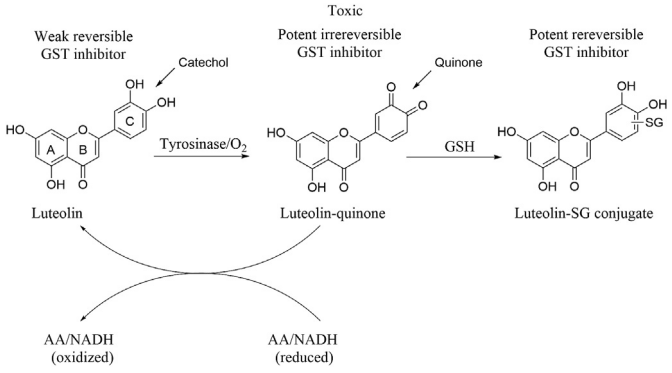

Scheme 1. Summary of tyrosinase mediated selective bio-activation of luteolin. Luteolin is selectively bio-activated to luteolin-quinone in presence of tyrosinase. In the presence of glutathione, luteolin-quinone is further metabolized to luteolin-SG-conjugate. Luteolin-quinone is toxic towards the melanoma cells. GST is responsible for enhancing drug resistance in melanoma cells. Luteolin-quinone inhibits GST in irreversible while luteolin-SG-conjugate inhibits GST in reversible mechanism. Luteolin in absence of tyrosinase inhibits GST in reversible fashion at higher concentrations (≥40 μM), hence, a weaker inhibitor. Catechol group is the aromatic ring with two adjacent OH groups on ring C.

2. Materials and methods

2.1. Materials

All the reagents and solvents used in this study including glutathione (GSH), 1-chloro-2,4-dinitrobenzene (CDNB), glutathione S-transferase (GST), 2-nitro-5-thiobenzoic acid (DTNB), were of analytical grade with the highest degree of purity and were purchased from Sigma–Aldrich, St. Louis, MO or Fisher-Scientific, Pittsburgh, PA. For this study mushroom tyrosinase was used since purified human tyrosinase is not available for commercial purchase. The GST π enzyme was derived from human placenta. Because the compounds were dissolved in DMSO, the final concentration of DMSO was 1% v/v in cell culture media of the cells treated with various compounds. Therefore, the media for control cells contained 1% v/v DMSO in the experiment. The glutathione was dissolved in phosphate buffered saline (PBS) (Cat. No. SH30526.02) from Thermo Scientific (Hyclone®).

2.2. Cell line and culture conditions

The human melanoma SK-MEL-28 cell line for this study was obtained from ATCC®, Manassas, VA. Modified Eagle Medium Alpha (MEMα) (Cat. no. 32571-036) and fetal bovine serum (FBS) (Cat. No. 10082-139) were purchased from American Type Culture Collection (ATCC®), Manassas, VA. Versene (1×, 0.2 g EDTA 4Na/L in phosphate-buffered saline) (1:5000 Cat. No. 15040-066) was obtained from Invitrogen, Grand Island, NY.

2.3. UV–vis spectroscopy of enzyme mediated oxidation

The luteolin oxidation by enzyme tyrosinase was analyzed by a previously described UV–vis spectroscopy method [17]. Reaction mixture contained luteolin (200 μM) and tyrosinase (20 U/mL) and spectra was obtained every five minutes with or without glutathione (500 μM) by a GBC UV–visible spectral spectrophotometer (GBC Scientific, Victoria, Australia). The control spectrum was obtained by adding luteolin (200 μM) to 0.1 M phosphate buffer (pH 6.5) containing 1 mM diethylenetriaminepentaacetic acid (DETAPAC). In same manner spectra were recorded in presence of ascorbic acid (200 μM) and nicotinamide adenine dinucleotide (NADH) (200 μM).

2.4. Rate of AA and NADH oxidation

The luteolin is metabolized by tyrosinase enzyme which leads to oxidation of ascorbic acid [18] and NADH. The rate of oxidation of these compounds was measured as previously described [3,19]. The reaction mixture consisted of tyrosinase (5 U/mL), luteolin (100 μM) and AA (50 μM) in the presence and absence of GSH (200 μM) made to a volume of 2 mL in phosphate buffer (0.1 M, pH 7.4, DETAPAC 1 mM) [19]. Similar experiments were performed with NADH (200 μM). The oxidation of AA and NADH was analyzed at 266 nm and 340 nm, respectively. The 4-hydroxyanisole (4-HA) is known to be a substrate for tyrosinase. Following equation was used to compute oxidation rate [3]:

$$\text{Rate of AA oxidation } (\mu\text{M/min/Unit tyrosinase}/\mu\text{M phenolic agent}) = [\text{change in AA absorbance}/\text{initial AA absorbance}] \times [\text{AA } (\mu\text{M})/\text{Luteolin}(\mu\text{M})] \times [1/\text{tyrosinase}(\text{U/mL})] \times [1/\text{time}]$$

The rate of NADH oxidation was computed in the similar fashion.

2.5. Tyrosinase mediated glutathione depletion assay

The extent of GSH depletion due to oxidation of test compound by tyrosinase enzyme was quantified by a previously described method [4]. Reaction mixture contained tyrosinase (20 U/mL), luteolin (200 μM) and GSH (500 μM) in phosphate buffer (0.1 M, pH 6.5) in a final volume of 2 mL. The mixture was incubated for 30 min at 37 °C. A 250 μL aliquot from the reaction mixture was added to trichloroacetic acid (25 μL; 30% w/v), vortexed and kept at room temperature for 5 min. Then, 100 μL aliquot was added to tube containing Ellman's reagent (DTNB) (25 μL; 2 mg/mL) and Tris/HCl buffer (875 μL; 0.1 M, pH 8.9). The absorbance of mixture was obtained by taking optical density (O.D.) at 412 nm by spectrophotometer [20]. The depletion of glutathione indicates the tyrosinase mediated oxidation of test compound. Similarly, enzymatic oxidation of 4-HA was measured as positive control [19].

2.6. The inhibition of human placenta GST π by luteolin

Placenta GST π inhibition by luteolin was analyzed by UV–vis spectroscopy method. Human placenta GST π was used for this experiment and throughout the study and inhibition was measured by the method of Tuna et al. [21]. The reaction mixture consisted of glutathione (1 mM) and CDNB (1 mM) and 0.1 U/mL human placenta GST in potassium phosphate buffer (100 mM, pH 6.5) to a final volume of 2.5 mL [21]. Different concentrations of luteolin (5, 10 and 25 μM) were used to study GST inhibition. The time scan spectra were taken for 5 min at 340 nm by GBC UV–visible spectral spectrophotometer (GBC Scientific, Victoria, Australia). The absorbance difference between 1 min and 5 min was used to calculate the decrease in GST activity, which indicates the extent of GST inhibition when compared to control. During the scan, reaction mixture was maintained at constant temperature of 25 °C.

2.7. GST inhibition by luteolin-quinone (formed in the presence of tyrosinase)

Enzyme tyrosinase metabolizes luteolin to luteolin-quinone. To study GST inhibition by luteolin-quinone; tyrosinase (20 U/mL), luteolin (25 μM), and GST (0.4 U/mL) were added to phosphate buffer (0.1 M, pH 6.5) to final volume of 2.5 mL and incubated for 30 min at 37 °C to enable luteolin metabolism by tyrosinase to luteolin-quinone. The reaction mixture was filtered through Millipore centrifugal filter units with 10 K molecular weight cutoff to separate GST from the reaction mixture (UFC801024, Amicon Ultra, Carrigtwohill, Ireland) to determine the reversible-irreversible nature of inhibition. Further, glutathione (1 mM) and CDNB (1 mM) [21] were added to the residual reaction mixture in the Millipore centrifugal filter unit and was made to final volume of 2.5 mL with phosphate buffer (0.1 M, pH 6.5). The spectra scan of this reaction mixture was obtained by UV–vis spectroscopy as mentioned in Section 2.7. Control solutions contained GST and/or GST/tyrsoinase in the absence of luteolin. GST activity of control samples was compared with test samples to determine the percentage GST inhibition by test compound.

2.8. GST inhibition by luteolin-SG conjugate (formed in the presence of GSH and tyrosinase)

Enzyme tyrosinase metabolizes luteolin to luteolin-SG conjugate in the presence of glutathione. The GST activity in presence of luteolin-SG conjugate was assessed by previously described CDNB method [21]. Tyrosinase (20 U/mL), luteolin (25 μM), glutathione (500 μM) and GST (0.4 U/mL) were added to phosphate buffer (0.1 M, pH 6.5) to final volume of 2.5 mL and incubated for 30 min at 37 °C to enable luteolin metabolism by tyrosinase in presence of glutathione to luteolin-SG conjugate. The reaction mixture was filtered through Millipore centrifugal filter units with 10 K molecular weight cutoff to separate GST from the reaction mixture (UFC801024, Amicon Ultra, Carrigtwohill, Ireland) to determine the reversible-irreversible nature of inhibition. Further, glutathione (1 mM) and CDNB (1 mM) were added to the residual reaction mixture in the Millipore centrifugal filter unit and was made to final volume of 2.5 mL with phosphate buffer (0.1 M, pH 6.5). The spectra scan of this reaction mixture was obtained by UV–vis spectroscopy as mentioned in Section 2.7. Control sample contained GST/glutathione/tyrsoinase in the absence of luteolin. GST activity of control samples was compared with test samples to determine the percentage GST inhibition by test compound.

2.9. The nature of GST inhibition: competitive and non-competitive GST inhibition by luteolin, luteolin-quinone, and luteolin-SG conjugate

The competitive, non-competitive and mixed nature of GST inhibition was determined by CDNB method [21] and the inhibition constant (K_i) of luteolin, luteolin-quinone, and luteolin-SG conjugate were derived by Lineweaver–Burk plots [22].

Tyrosinase enzyme (20 U/mL) was added onto a solution of luteolin (1 μM), and GSH (1 mM) in phosphate buffer (0.1 M, pH 6.5). The mixture was incubated for 30 min at 37 °C to allow the formation of luteolin-SG conjugate. Following this, GST (0.02 U/mL), CDNB (0.2–1 mM) were added to the solution mixture and UV–vis spectra of sample was obtained at 340 nm for 5 min. During scan, temperature of sample was maintained at 25 °C by circulating temperature maintained water in water-jacket cuvette, powered by a pump. The rate of reaction was determined by calculating difference in absorbance between 5 and 1 min. These experiments were conducted on three different days to consider between-day variation. All reagents were prepared fresh on the day of study. The mean of results obtained on three different days was used to construct Lineweaver–Burk plot and nature of inhibition was established using these plots. Inhibitory constant values were derived from Michaelis–Menton constants, maximum reaction rates and concentration of inhibitory species [22].

The control sample consisted of GSH (1 mM), GST (0.02 U/mL) and CDNB (0.2–1 mM). The concentration of CDNB varied (0.2–1 mM) when character of GST inhibition was assessed with respect to CDNB. Similarly, the GSH concentration varied (0.2–1 mM), when GST inhibition was determined with respect to GSH.

In similar manner, the nature of GST inhibition by luteolin-quinone (0.1 μM) and luteolin (100 μM) was determined in presence of GSH or CDNB. For quinone experiment, sample mixture was incubated for 5 min at 30 °C, while for experiments involving only luteolin, the sample mixture was not incubated with tyrosinase and GSH.

2.10. Calculations of inhibitory constants

The inhibitory constants (K_i) of inhibition were determined from Line-weaver Burk plots using the following equations [22].

$$\text{Competitive Inhibition}: \; K_i = K_m \times [I] \Big/ \left(K_m^* - K_m\right)$$

$$\text{Non} - \text{competitive Inhibition}: \; K_i = V_{\max}^* \times [I] \Big/ \left(V_{\max} - V_{\max}^*\right)$$

Mixed Inhibition:

(a) $K_i = V^*_{max} \times K_m \times [I]/\{(V_{max} \times K^*_m) - (V^*_{max} \times K_m)\}$
(b) $K'_i = V^*_{max} \times [I]/(V_{max} - V^*_{max})$

here, K_m and K^*_m values are Michaelis–Menton constants, V_{max} and V^*_{max} values are maximum reaction rates, and K_i and K'_i are the inhibition constants. Thus two inhibition constants; K_i (inhibitor binding to enzyme) and apparent K'_i (apparent K_i when inhibitor binds with ES complex) were calculated for mixed inhibition using formulas provided in 'Biochemistry' by Garrett & Grisham 2005 [23]. The K_m and V_{max} represents the constant for the assay performed in absence of inhibitor. While, K^*_m and V^*_{max} represents the constant for the assay performed in presence of inhibitor (luteolin, luteolin-quinone, or luteolin-SG conjugate). Concentration of inhibitor is represented by [*I*] in above formulas.

2.11. The time and concentration dependent inhibition of GST by luteolin in the presence of tyrosinase

To appreciate time and concentration dependent inhibition of GST by luteolin, tyrosinase (20 U/mL) and luteolin (0.25–2.50 μM) were added to GST (2 U/mL) to a final volume of 1 mL in phosphate buffer (0.1 M, pH 6.5). The reaction mixture was incubated at 37 °C with shaking (100 rpm) and tested for GST activity at 30 min, 1 h, 2 h, 4 h, 8 h, 24 h and 48 h. An aliquot of 62.5 μL from reaction mixture was added to GSH (1 mM) and CDNB (200 μM) and made to final volume of 2.5 mL with phosphate buffer (0.1 M, pH 6.5). The time scan spectra were taken for 5 min at 340 nm as described in Section 2.7 and difference in absorption at 1 and 5 min denotes GST activity. The 3 controls were used in this experiment consisted of GST, GST + tyrosinase, and GST + luteolin.

2.12. Depletion of intracellular GSH by luteolin

Exponentially growing 70% confluent cells were suspended in MEMα media enriched with (10%) FBS at 1×10^6 cells/mL in 24-well plates. Following incubation at 37 °C for 3 h, an additional 1 mL media containing varying concentrations of luteolin was added and cells were further incubated for 1, 2 and 3 h, respectively. Quantity of intracellular GSH was assessed by a previously described method [3,24,25] in melanocytic SK-MEL-28 cells [17]. Results represent average of three independent experiments.

2.13. The inhibition of human SK-MEL-28 melanoma GST in cell homogenate by luteolin

Human SK-MEL-28 melanoma cells were used to study inhibition of intracellular GST by luteolin [21,26]. The SK-MEL-28 cells were cultured in MEMα media supplemented by adding 10% FBS. Exponentially dividing 70% confluent cells were used for this experiment. GST inhibition in melanoma cells was assessed by CDNB method [21,27]. About 200,000 cells suspended in 500 μL media were sonicated for 3–5 seconds and subjected to centrifugation at 13,000 rpm for 15 min at 4 °C. The supernatant was collected and added onto mixture of glutathione (1 mM), different concentrations of luteolin (0.1, 0.25, 1, 2.5, 5, 10, 20, 40 and 80 μM), CDNB (1 mM) and tyrosinase (10 U/mL) made to final volume of 2.5 mL with phosphate buffer saline (100 mM, pH 6.5). The spectra scan of this reaction mixture was obtained by UV–vis spectroscopy as mentioned in Section 2.5.

2.14. Docking calculations

AutoDock tools 1.5.2 and AutoDock 4.0 [28,29] were used to predict the binding modes for both leutolin and leutolin-quinone with GST, in the presence of GSH. During the calculations, the protein and ligands were treated as rigid groups. The predicted bound configuration with the lowest free energy of binding was chosen for each ligand. Crystal structure of the wild-type GST (PDB ID 11GS) [30,31] was applied for this study.

2.15. Statistical analysis

All the experiments were performed with at least three replicates. Results are presented as mean ± SD.

3. Results

3.1. UV–vis spectroscopy of tyrosinase mediated enzymatic oxidation of luteolin

The advancement of luteolin oxidation by tyrosinase enzyme was recorded by UV–vis spectrophotometer. After addition of tyrosinase, as scans were repeated at 6 min intervals, a progressive decrease was observed in luteolin peaks at 350 nm (Fig. 1A). Moreover, the formation of new peaks was observed at 240–270 nm, indicating the generation of new products of oxidation/metabolism process with different absorption characteristics (Fig. 1A) [32,33]. However, addition of GSH before commencing oxidation by tyrosinase prevented the formation of new oxidation product for luteolin as evident from the absence of new peaks (Fig. 1B). These results suggest that luteolin is a substrate for tyrosinase enzyme forming an o-quinone product, which could react with glutathione (Fig. 1B). Distinct peaks are observed in spectra of ascorbic acid (AA) and NADH at 266 nm and 340 nm respectively. The absorbance at these spectra at 266 nm and 340 nm were decreased significantly upon addition of luteolin and tyrosinase, indicating the oxidative depletion of AA and NADH by luteolin-quinone (Fig. 1C and E). When GSH was added to reaction mixture, the depletion of AA and NADH was significantly reduced (Fig. 1D and F). Our findings indicate that luteolin-quinone reacts with GSH, sparing AA and NADH oxidation. Luteolin alone produced a stable spectrum leading to conclusion that it does not undergo auto-oxidation over the course of experiment.

3.2. Rate of AA and NADH oxidation

The rate of AA, GSH, and NADH depletion indicated the extent of luteolin oxidation by tyrosinase (Fig. 2A and B). The extent of depletion for three compounds were, AA > NADH > GSH. The GSH was able to significantly prevent the oxidation of AA and NADH.

Rate of AA and NADH oxidation were found to be 11 and 12 (μM/min/Unit tyrosinase/μM phenolic agent). In the presence of GSH the rate of oxidation of AA and NADH oxidation reduced to 1 and 2 (μM/min/Unit tyrosinase/μM phenolic agent), respectively.

3.3. Tyrosinase mediated glutathione depletion assay

Tyrosinase mediated metabolism of luteolin produced depletion of GSH in *in-vitro* experiments. This GSH depletion could be used as a biomarker of luteolin oxidation. The incubation with luteolin for 15, 30 and 60 min resulted in depletion of 110%, 137% and 170% GSH (equivalent to 1.1, 1.4 and 1.7 mole ratio), respectively (Fig. 3). This finding suggests that luteolin can form a mono and bi-glutathione conjugates as the time progress in the reaction. The GSH depletion by tyrosinase mediated oxidation of 4-HA (4-hydroxyanisole) was used as positive control (data not shown) [34]. Negligible glutathione was lost in the absence of tyrosinase enzyme (data not shown).

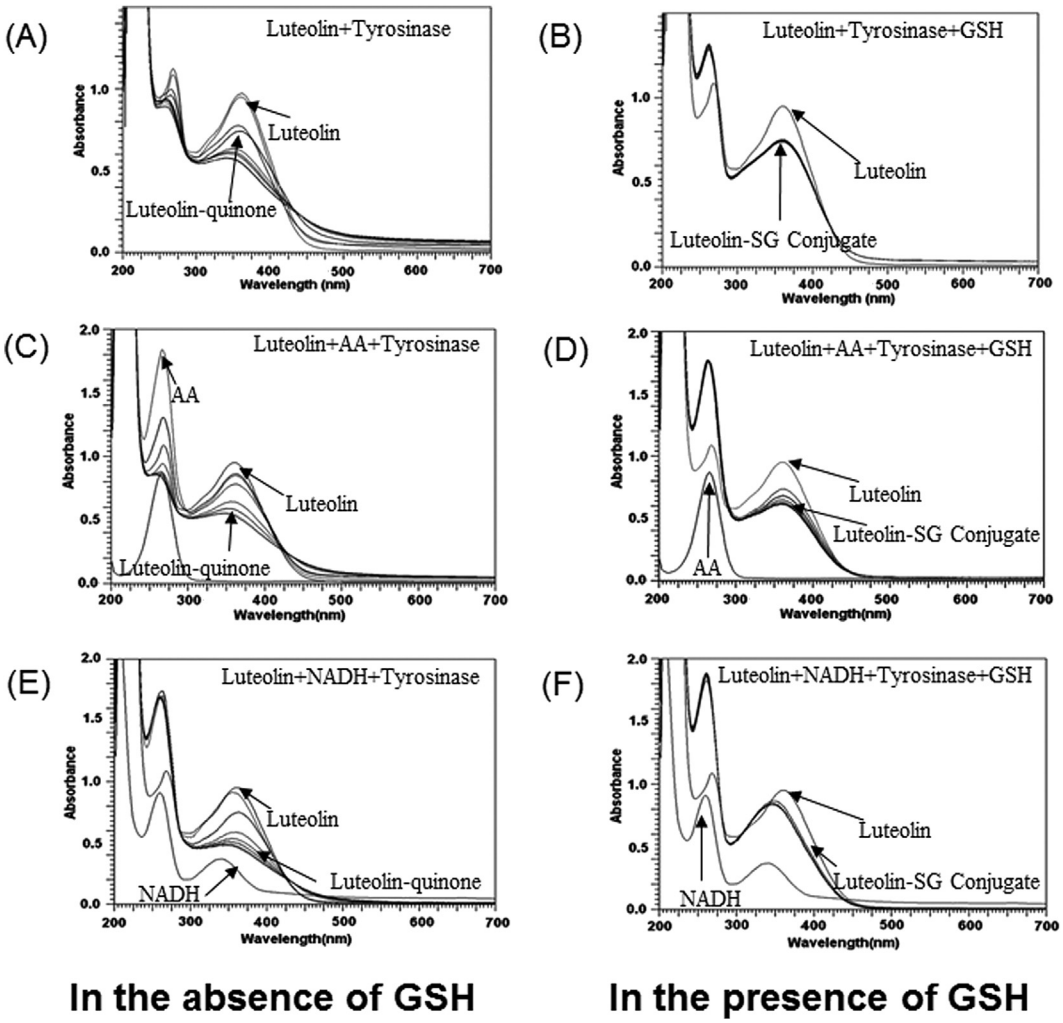

Fig. 1. UV–vis spectroscopy of tyrosinase mediated oxidation. (A) Oxidation of luteolin in the presence of tyrosinase. As luteolin is oxidized by tyrosinase, absorption peak at 350 nm was progressively diminished. (B) Upon addition of glutathione, new peaks were formed at 330 nm indicating the formation of glutathione conjugate with the oxidized product of luteolin. (C) Ascorbic acid (AA) forms distinctive peak at 266 nm. AA peak height diminished as repeated scans were taken at 5 min intervals indicating the AA oxidation by the oxidized product of luteolin. (D) Upon addition of glutathione, AA peak height did not decrease in repeated scans indicating the formation of a glutathione conjugate in the presence of GSH prevented AA oxidation. (E) NADH forms distinctive peak at 340 nm. NADH peak height diminished as repeated scans were taken at 5 min interval indicating the NADH oxidation by metabolized product of luteolin. (F) Upon addition of glutathione, NADH peak height did not change in repeated scans indicating that the luteolin glutathione conjugate is unable to oxidize NADH.

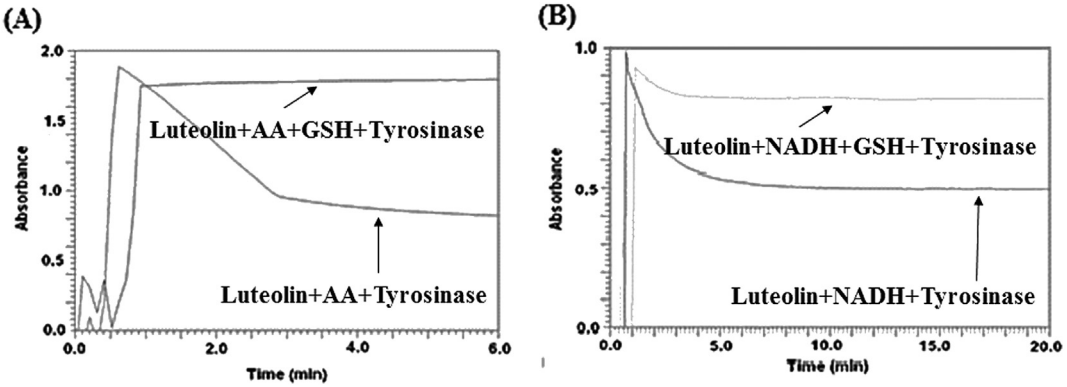

Fig. 2. The rate of AA and NADH oxidation. Kinetic scans for luteolin oxidation by tyrosinase. The oxidation of AA (A) and NADH (B) by luteoline in the presence of tyrosinase was recorded at 266 nm and 340 nm, respectively. Addition of GSH before adding tyrosinase diminished the rate of oxidation of AA and NADH, indicating that the oxidized product of luteolin reacted with glutathione preferentially.

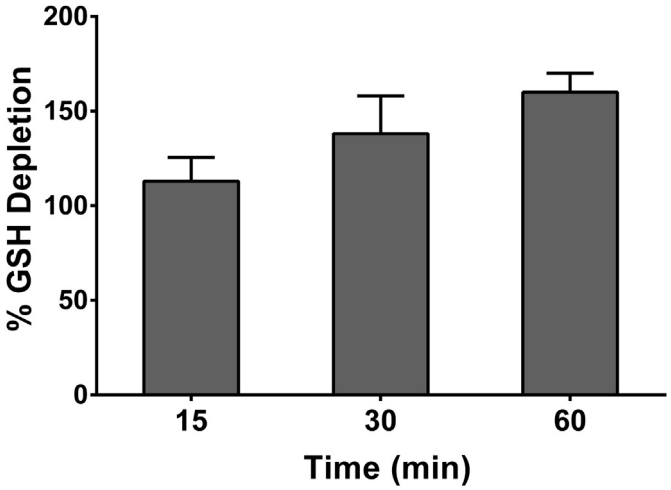

Fig. 3. Tyrosinase mediated GSH depletion by luteolin. The GSH depletion is demonstrated as % of control at different time points.

3.4. The inhibition of human placenta GST by luteolin, luteolin-quinone and luteolin-SG conjugate

Luteolin in absence of tyrosinase enzyme was unable to inhibit the activity of GST enzyme at concentrations less than 25 μM. Nevertheless, it was able to inhibit GST activity to more than 90% at 100 μM concentration. Neither 4-HA (50 μM), a substrate for tyrosinase [19] nor tyrosine (25–50 μM), a natural substrate of tyrosinase [34], were able to produce significant inhibition of GST activity. Contrary to this, luteolin-quinone, bioactivation product of luteolin formed by tyrosinase enzyme, showed about 85–90% inhibition at 10 and 20 μM concentrations. While GST inhibition by other tyrosinase substrates such as 4-HA-quinone (50 μM) and tyrosine-quinone (50 μM) was less than 20%.

Luteolin-SG conjugate, the bio-activation product of luteolin catalyzed by tyrosine in the presence of GSH, inhibited the GST activity by 88–95% at concentrations ranging from 5 to 25 μM (Fig. 4). The 4-HA-SG conjugate and tyrosine-SG conjugate did not significantly inhibit GST activity at similar concentrations (data not shown). The extent of GST inhibition in descending order was luteolin-quinone >> luteolin-SG-conjugate >>> luteolin.

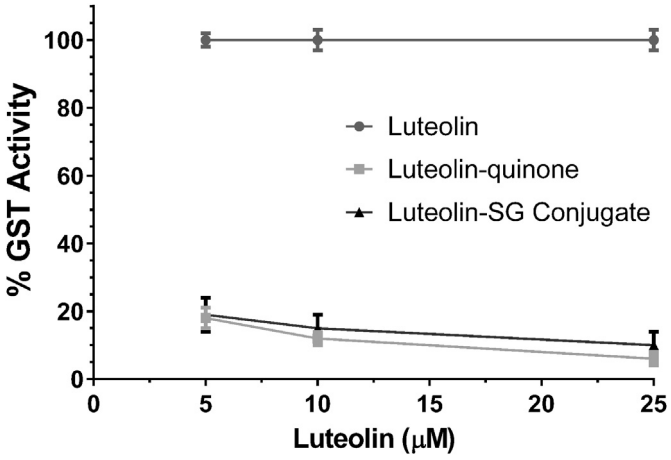

Fig. 4. Inhibition of human placenta GST. The inhibitory effects of luteolin, luteolin-quinone and luteolin-SG conjugate on human placenta GST. Luteolin-SG conjugate and luteolin-quinone at 5–25 μM demonstrated 88–95% GST inhibition. Luteolin alone at this concentration exhibited negligible GST inhibition.

3.5. Irreversible and reversible inhibition of GST by luteolin-quinone, luteolin-SG conjugate and luteolin

The GST was separated from reaction mixture by filtering the solution mixture through 10 K Millipore filter. Luteolin-SG conjugate (10 μM) was able to significantly inhibit GST (Fig. 5A), the GST activity was recovered after filtering the reaction mixture through 10 K Millipore filter (Fig. 5B), suggesting that luteolin-SG conjugate inhibited GST in a reversible non-covalent binding manner. Similarly luteolin-quinone exhibited considerable GST inhibition. Filtration of reaction mixture by 10 K Millipore filter did not recover the GST activity for luteolin-quinone leading to conclusion that GST was inhibited by luteolin-quinone by covalent binding in an irreversible manner. No inhibition of enzymatic activity of GST was evident in the presence of tyrosinase enzyme alone (data not shown).

3.6. Competitive and non-competitive GST inhibition by luteolin, luteolin-quinone, luteolin-SG conjugate

The activity of GST enzyme was determined with respect to substrates CDNB and GSH (0.2–1 mM) to decipher the mechanism of GST inhibition by luteolin, luteolin-quinone, luteolin-SG conjugate.

Double reciprocal plot of 1/rate versus 1/[GSH] lines in presence and absence of inhibitor did not intercept at 1/[rate] axis or 1/[GSH] axis, indicating the mixed inhibition of GST by luteolin with K_i of

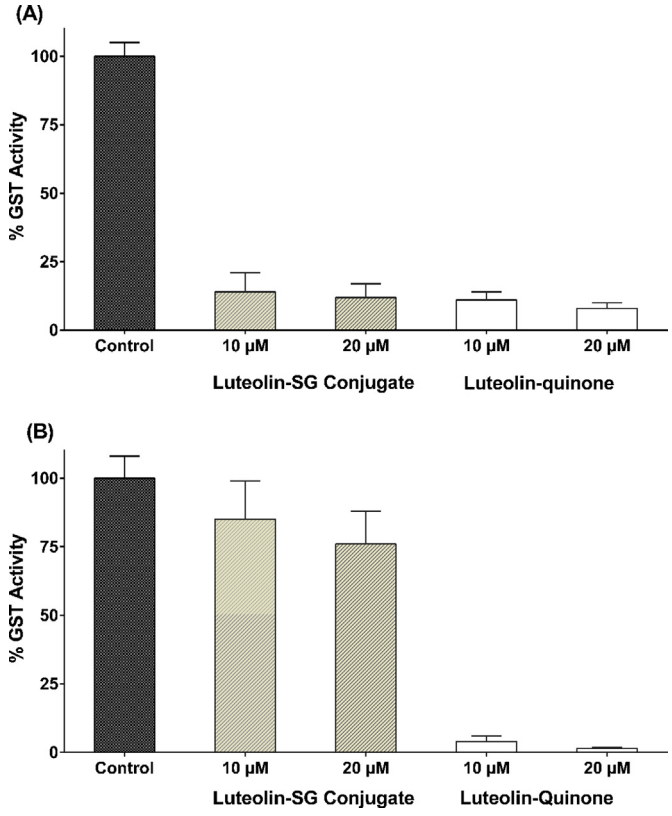

Fig. 5. Reversible and irreversible inhibition of human placenta GST. (A) Activity of human placenta GST before filtration through 10 K Millipore filter. Luteolin-SG conjugate and luteolin-quinone demonstrated significant GST inhibition at both 10 and 20 μM concentrations. (B) Activity of human placenta GST after separating the GST by filtration through 10 K Millipore filter. Note, irreversible inhibition of human placenta GST. Luteolin-quinone produced significant irreversible inhibition of GST by luteolin-quinone; however the GST activity was recovered after removing luteolin-SG conjugate through filtration, indicating luteolin-SG conjugate was not bound to GST covalently.

53 μM and K_i' of 97 μM (Fig. 6A) with respect to GSH. Luteolin-quinone demonstrated a mixed inhibition with 0.02 μM K_i and 0.05 μM K_i' (Fig. 6B). Luteolin-SG conjugate demonstrated competitive inhibition as the lines with inhibitor and without inhibitor intercepted y-axis (1/rate axis) with a K_i of 0.74 μM (Fig. 6C; Table 1).

Luteolin inhibited GST, with respect to CDNB (0.2–1 mM), in a non-competitive fashion with K_i of 38 μM (Fig. 6D), while luteolin-quinone demonstrated mixed inhibition with K_i value of 0.04 μM and K_i' value of 0.08 μM (Fig. 6E). The competitive inhibition was found to be generated by luteolin-SG conjugate with respect to CDNB with 0.58 μM K_i (Fig. 6F; Table 1). Ethacrynic acid, a known inhibitor of GST [35], demonstrated competitive inhibition with respect to CDNB and non-competitive inhibition with respect to GSH with K_i values of around 5 μM and 10 μM, respectively (data not shown).

Table 1
Summary data for GST inhibition and mechanism of inhibitions. Nature of inhibition of GST inhibition by luteolin, luteolin-quinone, and luteolin-SG conjugate with respect to CDNB and GSH. In mixed inhibition, inhibitor binds to both enzyme (E) and enzyme substrate complex (ES) with different affinities. Thus two inhibition constants; K_i (inhibitor binding to enzyme) and apparent K_i' (when inhibitor binds to ES complex) were calculated for mixed inhibition using formulas provided in 'Biochemistry' by Garrett & Grisham 2005 [23].

Inhibitor	Inhibition	K_i (μM)	K_i' (μM)
With respect to GSH (0.2–1 mM)			
Luteolin	Reversible mixed	53	97
Luteolin-quinone	Irreversible mixed	0.02	0.05
Luteolin-SG Conjugate	Reversible competitive	0.74	Not applicable
With respect to CDNB (0.2–1 mM)			
Luteolin	Reversible non-competitive	38	Not applicable
Luteolin-quinone	Irreversible mixed	0.039	0.08
Luteolin-SG Conjugate	Reversible competitive	0.58	Not applicable

3.7. Time and concentration dependent inhibition of GST by luteolin

Luteolin in the presence of tyrosinase formed luteolin-quinone which inhibited GST both in a concentration- and time-dependent manner (Fig. 7). Luteolin was tested at various concentrations of 0.25, 0.625, 1.25, and 2.50 μM. GST inhibition was measured at 0.5, 1, 2, 4, 8 and 24 h incubation. At 0.25 μM

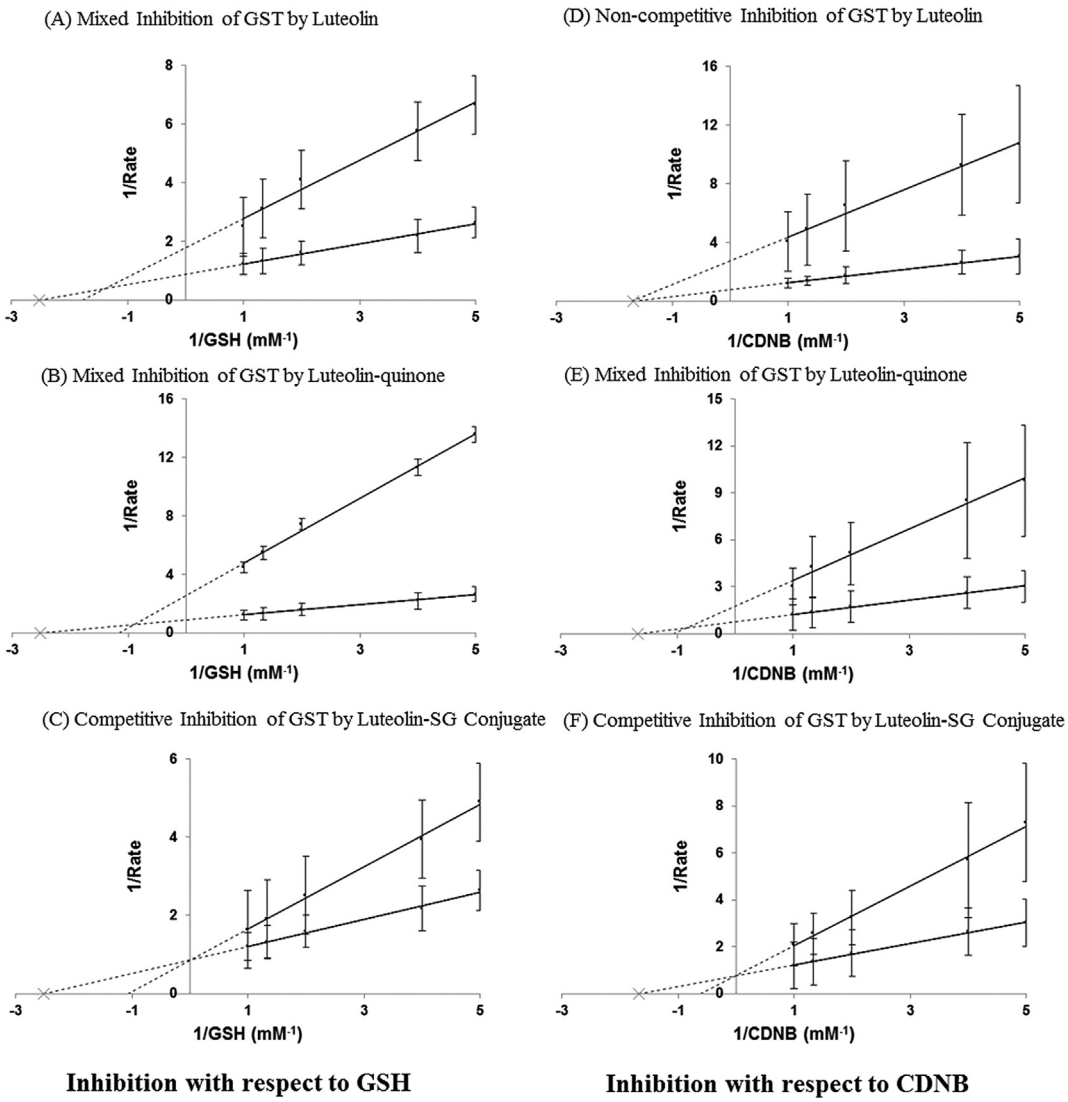

Fig. 6. Lineweaver–Burk plots of the GST inhibition by luteolin, luteolin-quinone and luteolin-SG conjugate. (A) Mixed GST inhibition by luteolin with respect to GSH. (B) Mixed GST inhibition by luteolin-quinone with respect to GSH. (C) Competitive GST inhibition by luteolin-SG conjugate with respect to GSH. (D) Non-competitive GST inhibition by luteolin with respect to CDNB. (E) Mixed GST inhibition by luteolin-quinone with respect to CDNB. (F) Competitive GST inhibition by luteolin-SG conjugate with respect to CDNB.

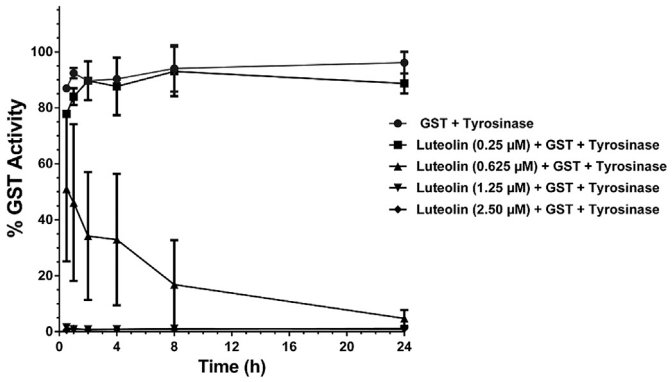

Fig. 7. Time and concentration dependent inhibition of GST by luteolin. Luteolin in presence of tyrosinase inhibited GST both in a concentration- (0.25–2.50 μM) and time-dependent manner (0.5–24 h).

concentration luteolin-quinone inhibited 21% GST activity. The inhibition diminished as incubation progressed and only 9% inhibition was observed after 24 h. At 0.625 μM luteolin-quinone, 49% of GST activity was inhibited at 0.5 h time point and inhibition increased progressively to 95% at 24 h incubation time. At higher luteolin-quinone level of 1.25 and 2.50 μM > 99% inhibition was observed at 0.5 h and all other subsequent time points.

3.8. Intracellular GSH depletion in human melanoma SK-MEL-28 cells

40 μM luteolin depleted 16% intracellular GSH at 1 h incubation with human melanocytic SK-MEL-28 melanoma cells. Depletion increased to 20% and 24% after 2 h and 3 h incubation, respectively. At 80 μM luteolin, GSH depletion was 20%, 22% and 27% at 1 h, 2 h, and 3 h, respectively. At 200 μM luteolin caused GSH depletion of 32%, 35% and 37%, respectively (Fig. 8). Luteolin caused concentration-dependent and time-dependent GSH depletion in human melanoma cells. Most of the depleted GSH occurred at first hour of incubation.

3.9. Inhibition of GST in human SK-MEL-28 melanoma cell homogenates by luteolin

Luteolin (0.1–80 μM), in the presence of tyrosinase, demonstrated significant degree of selective inhibition (0–97%) of GST in SK-MEL-28 cell homogenate (Fig. 9). This inhibition was found to be concentration dependent. The observation that luteolin at minimal concentration of 1 μM produced 50% inhibition of GST indicates the GST inhibitory potency of luteolin in presence of tyrosinase. Compared to this both 4-HA and tyrosine, known tyrosinase substrates [36] produced negligible GST inhibition at similar concentrations (data not shown).

3.10. Docking calculations

The docking results show that both luteolin and luteolin-quinone dock perfectly to the H-site in the GST active site in the presence of GSH. However, the calculated free energy of binding significantly favors luteolin-quinone over luteolin.

CYS101 site is a known catalytic site of GST [37]. It is a cysteine group which first reacts reversibility with GST substrates facilitating the reaction of this intermediate with GSH. After reaction of intermediate with GSH, the CYS101 will be released to regenerate functional GST. On the other hand luteolin-quinone when in close proximity of the catalytic CYS101 site (Fig. 10), reacts irreversibility with thiol group of CYS101, suggesting permanent inactivation of the enzyme. The fact that the GST activity is not regenerated indicates that the reaction with CYS101 is irreversible and GSH cannot release CYS101.

4. Discussion

Luteolin is a bioflavonoid and its antioxidant, anti-inflammatory properties and chemopreventive use in traditional medicine were reported previously [38,39]. Many studies have affirmed its properties such as induction of cell growth arrest, activation of caspase 7, apoptosis of multi-drug resistance proteins [40], which potentially could be useful in treatment of different types of cancer.

Our lab has focused on tyrosinase as a molecular target in melanoma for past 10 years. We previously showed that a number of compounds that are oxidized by tyrosinase such as acetaminophen and caffeic acid phenyl ester [41] are highly and selectively toxic towards melanoma cells both *in-vivo* and *in-vitro* [3,5,17,42]. Because tyrosianse is found abundantly in melanoma, using a tyrosianse targeted approach offers an advantage for selective toxicity in melanoma versus non-melanoma cancers.

Many factors such as GST causes drug resistance to chemotherapy in cancer cells rendering many therapeutic approaches ineffective [2,25,43]. GST is highly expressed in melanocytic cells

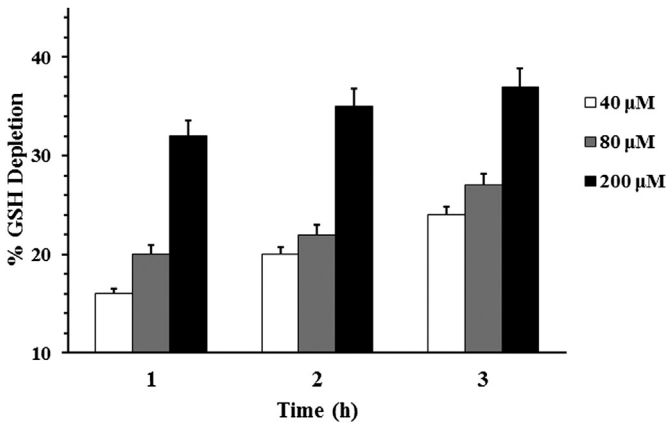

Fig. 8. Intracellular GSH depletion in human melanoma SK-MEL-28 cells. Luteolin (40–200 μM) demonstrated time and concentration dependent depletion of intracellular GSH in human melanoma SK-MEL-28 cells.

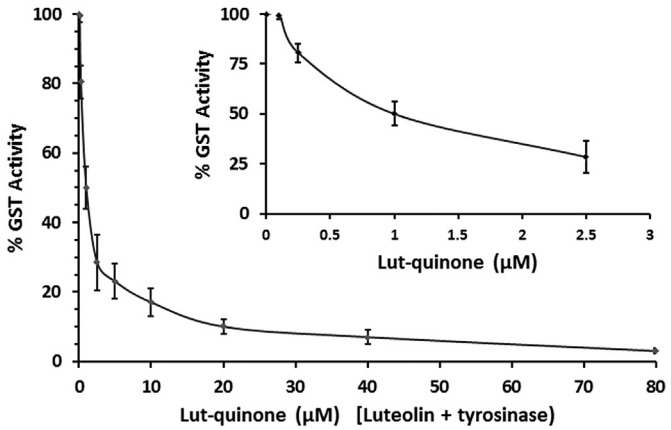

Fig. 9. Inhibition of the human SK-MEL-28 melanoma GST by luteolin. Luteolin (0.1–80 μM) demonstrated concentration-dependent GST inhibition ranging from 0 to 97% in human melanoma SK-MEL-28 cells homogenates.

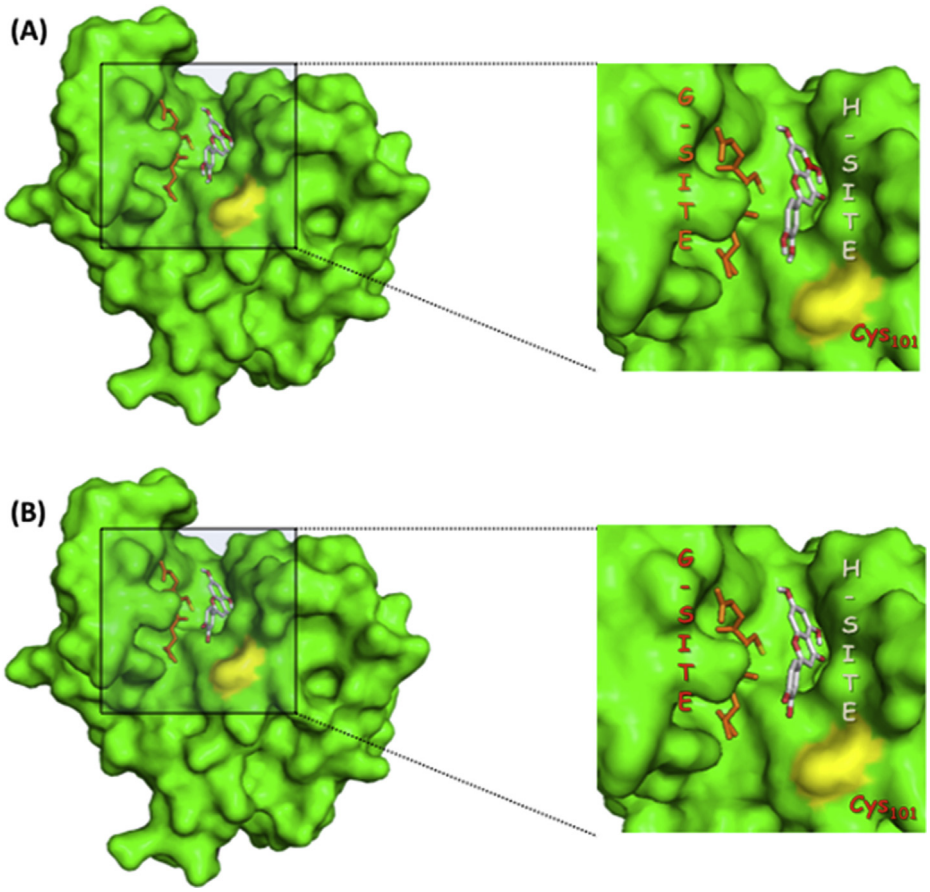

Fig. 10. Computational docking of luteolin and luteolin-quinone in the active sites of GST (green surface), in the presence of GSH (orange stick). (A) GSH occupies the G site and luteolin (gray and red stick) overlaps with the H site in the active site of GST. The sulfur atom in GSH and residue CYS_{101} are shown in yellow color. (B) GSH occupies the G site and luteolin-quinone (gray and red stick) overlaps with the H site in the active site of GST. The sulfur atom in GSH and residue CYS_{101} are shown in yellow color. The quinone, the reactive group of luteloin–quinone, is close to CYS_{101} in active site. The figures on the right are close ups of the active site highlighted by the box. (For interpretation of the references to colour in this figure legend, the reader is referred to the web version of this article.)

and is known to contribute to drug resistance [44,45] by converting active drug to inactive form. GST isoform GSTπ catalyzes the glutathiolynation of cellular proteins, thus provides protection from oxidative stress. Inhibition of GSTπ could be an effective strategy to reduce drug resistance in melanoma. GSTπ contains thiol molecule which could be depleted by flavonoid [46]. Unsaturated aldehydes and ketones can alter the Cys47 residue of GSTπ leading to loss of GST function [18,47,48]. Many studies reported GST inhibition by glutathione conjugates [49,50]. For instance, glutathione conjugated form of anti-cancer drug doxorubicin demonstrated GST inhibition and enhanced cytotoxicity towards cancer cell [49]. Hence, it would be interesting to identify compounds capable of selectively inhibiting GST in melanoma cancer cells as supplementary drug along with main anti-cancer drug to enhance therapeutic outcome. Previously, we have reported that CAPE is a substrate of tyrosinase and CAPE-quinone and CAPE-SG-conjugate significantly inhibited GST in human and mouse melanoma cell lines [26].

In this study, with the hope of identifying a lead compound, we screened rutin, querecetin, catechin and luteolin for their ability to inhibit GST in the presence of tyrosinase. All the four compounds were reported previously to be substrates for tyrosinase [51]. The depletion of AA, GSH, and NADH are used as the biomarkers of luteolin oxidation by tyrosinase. In addition, luteolin via auto-oxidation in presence of oxygen and in biological specimens due to one electron reduction can potentially form superoxide and hydrogen peroxides (not investigated in this study, for additional discussion see Refs. [5,52]).

Among rutin, querecetin, catechin and luteolin, only luteolin was able to inhibit GST selectively at a low concentration in the presence of tyrosinase (Table 2). Many studies reported anti-cancer effects of luteolin. However, there is no report on effect of luteolin on GST activity. We have earlier showed that luteolin is able to form conjugate in presence of tyrosinase [52]. Hence, in the present study, we sought to investigate the GST inhibition by luteolin, luteolin-quinone and luteolin-SG-conjugate, the extent and nature of GST inhibition.

For the first time, we demonstrated that luteolin ($K_i \geq 40$ μM), luteolin-SG conjugate ($K_i < 0.75$ μM), and luteolin-quinone ($K_i < 0.05$ μM) considerably inhibit GST. We observed that luteolin is a weak GST inhibitor, while luteolin-SG-conjugate and luteolin-quinone are potent inhibitors of GST (Scheme 1, Tables 1 and 2). With respect to GSH, the Lineweaver–Burk plots indicated that the GST inhibition by luteolin and luteolin-quinone is mixed inhibition, while GST inhibition by luteolin-SG-conjugate is competitive in nature. With respect to CDNB substrate, GST inhibition by luteolin is non-competitive. Inhibition by luteolin-quinone and luteolin-SG-conjugate with respect to CDNB are mixed and competitive, respectively. Among the 3 species of intact luteolin, luteolin-SG conjugate, and luteolin-quinone, only the latter two have potential as drugs with $K_i < 1$ μM, which is potentially achievable *in-vivo* as therapeutic agents. The order of GST inhibition was luteolin-quinone >> luteolin-SG conjugate >>> luteolin.

The potency of GST inhibition by flavonoid is dependent on hydroxylation pattern and number of hydroxyl groups [53]. The

Table 2
Tyrosinase mediated bio-activation of a number of flavonoids and GST inhibition by their quinone and glutathione-conjugate products. Various flavonoids were screened to determine their bio-activation by tyrosinase and ability of their quinones and SG-conjugates to inhibit GST. Rutin, catechin, quercetin and luteolin were found to be metabolized by tyrosinase, hence, substrate for tyrosinase. Among these only luteolin-quinone and luteolin-glutathione conjugate were found to inhibit GST.

Compound	Tyrosinase substrate	GST inhibition by compound alone	GST inhibition by quinone	GST inhibition by conjugate
4-HA	Yes	No	No	No
Tyrosine	Yes	No	No	No
Rutin	Yes	No	96% inhibition	No
Catechin	Yes	No	99% inhibition	No
Quercetin	Yes	No	99% inhibition	No
Luteolin	Yes	Weak inhibitor	99% inhibition	80% inhibition

presence of a catechol group (two −OH groups) and unsaturated bonds makes luteolin a potential candidate to inhibit GST. In addition, luteolin mediated GSTπ depletion might be due to depletion of thiol content of GSTπ or enhancement of oxidative stress. Ethacrynic acid (EA) [36] is a known GSTπ inhibitor *in-vitro*. Presence of unsaturated carbonyl functional group at α, β positions makes EA a highly efficient GST inhibitor [54,55]. EA [32] is a known GSTπ inhibitor *in-vitro*. Presence of unsaturated carbonyl functional group at α, β positions, known as allyl ketone, makes EA a highly efficient GST inhibitor [46,47]. Hence chemicals with similar structures may potentially exhibit GST inhibition. Likewise, after oxidation by tyrosinase, luteolin structure is transformed to a chemical structure with carbonyl functional group adjacent to unsaturated bonds, similar to allyl ketone group, providing a similar reactive functional group which could inhibit GST. One should note that such allyl ketone structure is generated after metabolism by tyrosinase.

In addition, docking results suggest that both luteolin and luteolin-quinone dock perfectly to the H-site in the GST active site in the presence of GSH. However, the calculated free energy of binding significantly favors luteolin-quinone over luteolin, which is consistent with the lower K_i value observed in this study. One should also note that the reactive group of luteolin-quinone is close to the catalytic CYS101, suggesting a possible irreversible reaction with CYS101, supporting current experimental data that luteolin-quinone irreversibly inhibit GST.

One explanation that luteolin-SG conjugate inhibited GST in competitive and reversible manner with respect to both GSH and CDNB is that it fits well in the active site of GST and binds to both binding sites of GST. On the other hand, luteolin-quinone with low K_i of less than 0.05 μM inhibited GST via irreversible mixed mechanism. This could be because luteolin-quinone is chemically a highly reactive species, which could modify other cysteine groups outside the GST active site as well as CYS101 in active site (GST π has 4 cysteine groups). High K_i value for luteolin suggests that luteolin is a non-selective non-specific inhibitor of GST in the absence of tyrosinase and may bind non-specifically to other unspecified regions of GST (not investigated).

In addition to the role of GST in drug metabolism, one should note that xenobiotic metabolism and elimination is a complex process involving cross interaction of transcription factors, signaling pathways, phase I and phase II drug metabolizing enzymes and drug transporters. For instance, flavonoids have been reported to induce pregnane x receptor (PXR), which in turn induces activity of drug metabolizing enzymes such as CYP and GST [56], but none of these studies investigated the role of luteolin on the expression of PXR in presence of tyrosinase.

Although there are reports indicating that luteolin increases GST activity in intestine of control rat following 30 weeks administration [57,58], these observations were in healthy tissue and there are no tyrosinase activity present in intestine. Hence our findings are not in contrast with these studies, as the focus of this study was selective inhibition of GST in presence of tyrosinase present in melanoma cells.

In conclusion, we have shown for first time that in the presence of tyrosinase, luteolin is selectively bio-activated to its -quinone and -SG-conjugate metabolites. These bio-activated forms are capable of inhibiting GST at a very low concentration of 1 μM which is clinically achievable. Because high expression of tyrosinase and GST in melanoma, and that GST is partly responsible for resistance to anti-melanoma agents, suppression of GST activity by luteolin could be an effective strategy for anti-melanoma chemotherapy. These findings could help in designing more efficacious novel analogs for melanoma treatment.

Financial support

The work was supported in part by NCI/NIH 1R15CA122044-01A to M.M.

Conflict of interest

The authors state no conflict of interest.

Transparency document

Transparency document related to this article can be found online at http://dx.doi.org/10.1016/j.cbi.2015.08.011.

References

[1] A.X. Wang, X.Y. Qi, Targeting RAS/RAF/MEK/ERK signaling in metastatic melanoma, IUBMB Life 65 (9) (2013) 748–758.
[2] S.C. McNeely, et al., Sensitivity to sodium arsenite in human melanoma cells depends upon susceptibility to arsenite-induced mitotic arrest, Toxicol. Appl. Pharmacol. 229 (2) (2008) 252–261.
[3] N.M. Vad, et al., Efficacy of acetaminophen in skin B16-F0 melanoma tumor-bearing C57BL/6 mice, Int. J. Oncol. 35 (1) (2009) 193–204.
[4] M.Y. Moridani, et al., Metabolic activation of 4-hydroxyanisole by isolated rat hepatocytes, Drug Metab. Dispos. 30 (10) (2002) 1063–1069.
[5] S.K. Kudugunti, et al., Biochemical mechanism of caffeic acid phenylethyl ester (CAPE) selective toxicity towards melanoma cell lines, Chem. Biol. Interact. 188 (1) (2010) 1–14.
[6] S. Jagadeesh, S. Kyo, P.P. Banerjee, Genistein represses telomerase activity via both transcriptional and posttranslational mechanisms in human prostate cancer cells, Cancer Res. 66 (4) (2006) 2107–2115.
[7] C. Rodriguez-Caso, et al., Green tea epigallocatechin-3-gallate is an inhibitor of mammalian histidine decarboxylase, Cell Mol. Life Sci. 60 (8) (2003) 1760–1763.
[8] B.P. Burnett, et al., Flavocoxid inhibits phospholipase A2, peroxidase moieties of the cyclooxygenases (COX), and 5-lipoxygenase, modifies COX-2 gene expression, and acts as an antioxidant, Mediat. Inflamm. 2011 (2011) 385780.
[9] S. Mesia-Vela, F.C. Kauffman, Inhibition of rat liver sulfotransferases SULT1A1 and SULT2A1 and glucuronosyltransferase by dietary flavonoids, Xenobiotica 33 (12) (2003) 1211–1220.
[10] M. Merlos, et al., Flavonoids as inhibitors of rat liver cytosolic glutathione S-transferase, Experientia 47 (6) (1991) 616–619.
[11] R. Hayeshi, et al., The inhibition of human glutathione S-transferases activity by plant polyphenolic compounds ellagic acid and curcumin, Food Chem. Toxicol. 45 (2) (2007) 286–295.

[12] Y.Y. Wang, et al., Cross-resistance and glutathione-S-transferase-pi levels among four human melanoma cell lines selected for alkylating agent resistance, Cancer Res. 49 (22) (1989) 6185–6192.
[13] Y.S. Kim, et al., Luteolin suppresses cancer cell proliferation by targeting vaccinia-related kinase 1, PLoS One 9 (10) (2014) e109655.
[14] S.H. Park, et al., Luteolin induces cell cycle arrest and apoptosis through extrinsic and intrinsic signaling pathways in MCF-7 breast cancer cells, J. Environ. Pathol. Toxicol. Oncol. 33 (3) (2014) 219–231.
[15] M. Chi, et al., Insulin induces drug resistance in melanoma through activation of the PI3K/Akt pathway, Drug Des. Dev. Ther. 8 (2014) 255–262.
[16] J. Li, et al., Antifibrotic effects of luteolin on hepatic stellate cells and liver fibrosis by targeting AKT/mTOR/p70S6K and TGFbeta/Smad signalling pathways, Liver Int. 35 (4) (2015) 1222–1233.
[17] S.K. Kudugunti, et al., Efficacy of caffeic acid phenethyl ester (CAPE) in skin B16-F0 melanoma tumor bearing C57BL/6 mice, Invest. New Drugs 29 (1) (2011) 52–62.
[18] J.J. Bogaards, J.C. Venekamp, P.J. van Bladeren, Stereoselective conjugation of prostaglandin A2 and prostaglandin J2 with glutathione, catalyzed by the human glutathione S-transferases A1-1, A2-2, M1a-1a, and P1-1, Chem. Res. Toxicol. 10 (3) (1997) 310–317.
[19] M.Y. Moridani, Biochemical basis of 4-hydroxyanisole induced cell toxicity towards B16-F0 melanoma cells, Cancer Lett. 243 (2) (2006) 235–245.
[20] D. Gergel, A.I. Cederbaum, Interaction of nitric oxide with 2-thio-5-nitrobenzoic acid: implications for the determination of free sulfhydryl groups by Ellman's reagent, Arch. Biochem. Biophys. 347 (2) (1997) 282–288.
[21] G. Tuna, et al., Inhibition characteristics of hypericin on rat small intestine glutathione-S-transferases, Chem. Biol. Interact. 188 (1) (2010) 59–65.
[22] S. Oetari, M. Sudibyo, J.N. Commandeur, R. Samhoedi, N.P. Vermeulen, Effects of curcumin on cytochrome P450 and glutathione S-transferase activities in rat liver, Biochem. Pharmacol. 51 (1) (1996) 39–45.
[23] R. Garrett, C.M. Grisham, Biochemistry, third ed., Thomson Brooks/Cole, Belmont, Calif. ; London, 2005 xliii, 1086, 40, 41 pp.
[24] S. Awasthi, et al., Interactions of glutathione S-transferase-pi with ethacrynic acid and its glutathione conjugate, Biochim. Biophys. Acta 1164 (2) (1993) 173–178.
[25] P. Depeille, et al., Combined effects of GSTP1 and MRP1 in melanoma drug resistance, Br. J. Cancer 93 (2) (2005) 216–223.
[26] S.K. Kudugunti, et al., The metabolic bioactivation of caffeic acid phenethyl ester (CAPE) mediated by tyrosinase selectively inhibits glutathione S-transferase, Chem. Biol. Interact. 192 (3) (2011) 243–256.
[27] Y.R. Pokharel, et al., Potent protective effect of isoimperatorin against aflatoxin B1-inducible cytotoxicity in H4IIE cells: bifunctional effects on glutathione S-transferase and CYP1A, Carcinogenesis 27 (12) (2006) 2483–2490.
[28] G.M. Morris, et al., Automated docking using a Lamarckian genetic algorithm and an empirical binding free energy function, J. Comput. Chem. 19 (1998) 24.
[29] M.F. Sanner, Python: a programming language for software integration and development, J. Mol. Graph Model. 17 (1) (1999) 57–61.
[30] I. Quesada-Soriano, et al., Diuretic drug binding to human glutathione transferase P1-1: potential role of Cys-101 revealed in the double mutant C47S/Y108V, J. Mol. Recognit. 24 (2) (2011) 220–234.
[31] A.J. Oakley, et al., The glutathione conjugate of ethacrynic acid can bind to human pi class glutathione transferase P1-1 in two different modes, FEBS Lett. 419 (1) (1997) 32–36.
[32] S. Passi, M. Nazzaro-Porro, Molecular basis of substrate and inhibitory specificity of tyrosinase: phenolic compounds, Br. J. Dermatol. 104 (6) (1981) 659–665.
[33] S.K. Kudugunti, et al., Efficacy of caffeic acid phenethyl ester (CAPE) in skin B16-F0 melanoma tumor bearing C57BL/6 mice, Invest. New Drugs 29 (1) (2011 Feb) 52–62.
[34] J. Choi, et al., A newly synthesized, potent tyrosinase inhibitor: 5-(6-hydroxy-2-naphthyl)-1,2,3-benzenetriol, Bioorg. Med. Chem. Lett. 20 (16) (2010) 4882–4884.
[35] J.H. Ploemen, et al., Ethacrynic acid and its glutathione conjugate as inhibitors of glutathione S-transferases, Xenobiotica 23 (8) (1993) 913–923.
[36] G. Eisenhofer, et al., Tyrosinase: a developmentally specific major determinant of peripheral dopamine, FASEB J. 17 (10) (2003) 1248–1255.
[37] L.A. Ralat, R.F. Colman, Monobromobimane occupies a distinct xenobiotic substrate site in glutathione S-transferase pi, Protein Sci. 12 (11) (2003) 2575–2587.
[38] X. Cai, et al., The molecular mechanism of luteolin-induced apoptosis is potentially related to inhibition of angiogenesis in human pancreatic carcinoma cells, Oncol. Rep. 28 (4) (2012) 1353–1361.
[39] L.H. Zhu, et al., Luteolin reduces primary hippocampal neurons death induced by neuroinflammation, Neurol. Res. 33 (9) (2011) 927–934.
[40] P.S. Rao, et al., Luteolin induces apoptosis in multidrug resistant cancer cells without affecting the drug transporter function: involvement of cell line-specific apoptotic mechanisms, Int. J. Cancer 130 (11) (2012) 2703–2714.
[41] J. Cassidy, et al., First-line oral capecitabine therapy in metastatic colorectal cancer: a favorable safety profile compared with intravenous 5-fluorouracil/leucovorin, Ann. Oncol. 13 (4) (2002) 566–575.
[42] N.M. Vad, et al., Biochemical mechanism of acetaminophen (APAP) induced toxicity in melanoma cell lines, J. Pharm. Sci. 98 (4) (2009) 1409–1425.
[43] Y.C. Awasthi, et al., The non-ABC drug transporter RLIP76 (RALBP-1) plays a major role in the mechanisms of drug resistance, Curr. Drug Metab. 8 (4) (2007) 315–323.
[44] D. Schadendorf, et al., Membrane transport proteins associated with drug resistance expressed in human melanoma, Am. J. Pathol. 147 (6) (1995) 1545–1552.
[45] A. Moral, et al., Immunohistochemical study of alpha, mu and pi class glutathione S transferase expression in malignant melanoma. MMM Group. Multidisciplinary Malignant Melanoma Group, Br. J. Dermatol. 136 (3) (1997) 345–350.
[46] W.Y. Chen, et al., Protoapigenone, a natural derivative of apigenin, induces mitogen-activated protein kinase-dependent apoptosis in human breast cancer cells associated with induction of oxidative stress and inhibition of glutathione S-transferase pi, Invest. New Drugs 29 (6) (2011) 1347–1359.
[47] M.L. van Iersel, et al., Interactions of alpha, beta-unsaturated aldehydes and ketones with human glutathione S-transferase P1-1, Chem. Biol. Interact. 108 (1–2) (1997) 67–78.
[48] J.J. van Zanden, et al., Inhibition of human glutathione S-transferase P1-1 by the flavonoid quercetin, Chem. Biol. Interact. 145 (2) (2003) 139–148.
[49] T. Asakura, et al., Conformational change in the active center region of GST P1-1, due to binding of a synthetic conjugate of DXR with GSH, enhanced JNK-mediated apoptosis, Apoptosis 12 (7) (2007) 1269–1280.
[50] M.H. Lyttle, et al., Isozyme-specific glutathione-S-transferase inhibitors: design and synthesis, J. Med. Chem. 37 (1) (1994) 189–194.
[51] M.Y. Moridani, et al., Quantitative structure toxicity relationships for catechols in isolated rat hepatocytes, Chem. Biol. Interact. 147 (3) (2004) 297–307.
[52] G. Galati, et al., Peroxidative metabolism of apigenin and naringenin versus luteolin and quercetin: glutathione oxidation and conjugation, Free Radic. Biol. Med. 30 (4) (2001) 370–382.
[53] I. Bousova, et al., Naturally occurring flavonoids as inhibitors of purified cytosolic glutathione S-transferase, Xenobiotica 42 (9) (2012) 872–879.
[54] K.D. Tew, S. Dutta, M. Schultz, Inhibitors of glutathione S-transferases as therapeutic agents, Adv. Drug Deliv. Rev. 26 (2–3) (1997) 91–104.
[55] M.L. Iersel, et al., Inhibition of glutathione S-transferase activity in human melanoma cells by alpha,beta-unsaturated carbonyl derivatives. Effects of acrolein, cinnamaldehyde, citral, crotonaldehyde, curcumin, ethacrynic acid, and trans-2-hexenal, Chem. Biol. Interact. 102 (2) (1996) 117–132.
[56] H. Dong, et al., Flavonoids activate pregnane x receptor-mediated CYP3A4 gene expression by inhibiting cyclin-dependent kinases in HepG2 liver carcinoma cells, BMC Biochem. 11 (2010) 23.
[57] V. Manju, V. Balasubramaniyan, N. Nalini, Rat colonic lipid peroxidation and antioxidant status: the effects of dietary luteolin on 1,2-dimethylhydrazine challenge, Cell Mol. Biol. Lett. 10 (3) (2005) 535–551.
[58] V. Manju, N. Nalini, Chemopreventive potential of luteolin during colon carcinogenesis induced by 1,2-dimethylhydrazine, Ital. J. Biochem. 54 (3–4) (2005) 268–275.